Fragmentation of Negative Ions from Carbohydrates: Part 3. Fragmentation of Hybrid and Complex *N*-Linked Glycans

David J. Harvey
Department of Biochemistry, Glycobiology Institute, University of Oxford, Oxford, United Kingdom

Hybrid and complex *N*-linked glycans were ionized by electrospray in the presence of ammonium nitrate to give $[M + NO_3]^-$ and $[M + (NO_3)_2]^{2-}$ ions. Low energy collision-induced decomposition (CID) spectra of both types of ions were almost identical and were dominated by C-type glycosidic and cross-ring fragments, unlike the corresponding spectra of the positive ions that contained mainly B- and Y-type glycosidic fragments. Also, in contrast to fragments in the positive ion spectra, many of these ions appeared to be produced by single pathways following proton abstraction from specific hydroxy groups. Consequently, many ions were diagnostic for specific structural features. Such features included the composition of each of the two antennas, the presence or absence of a bisecting GlcNAc residue, and the location of fucose residues on the core GlcNAc residues and on the antennas. C-ions defined the sequence of the constituent monosaccharide residues. Detailed fragmentation mechanisms are proposed to account for several of the diagnostic ions. (J Am Soc Mass Spectrom 2005, 16, 647–659) © 2005 American Society for Mass Spectrometry

N-linked glycans, those attached to asparagine in glycoproteins, play a fundamental role in determining the biophysical properties of these compounds [1, 2]. Structural determination of these compounds has classically been performed by chemical or enzymatic release followed by exoglycosidase digestion, with products monitored by gel filtration chromatography [3] or, more recently, high-performance liquid chromatography (HPLC) [4–6] or matrix-assisted laser desorption/ionization (MALDI) mass spectrometry [7, 8]. More recently, in response to the introduction of mass spectrometers, such as the tandem quadrupole-time-of-flight instruments and problems with the commercial availability of exoglycosidases, an increasing number of investigators are using wholly mass spectrometric-based approaches for the analysis of these compounds (see for example the recent review by Zaia [9]).

Most of this work has concentrated on the production and fragmentation of positive ions although it has become apparent in recent years [10–16] that negative ion fragmentation produces complementary information and can, in many cases, yield less ambiguous spectra than those provided by positive ion spectra. We have recently investigated methods for producing stable negative ions from *N*-linked glycans and found that nitrate adducts, formed by electrospray from solvents containing small amounts of ammonium nitrate, yield intense negative ions that, on fragmentation, give several characteristic and diagnostic ions that are not present in the corresponding positive ion spectra [17]. Details of the fragmentation of high-mannose *N*-linked glycans, the early compounds in the biosynthesis of these compounds, were reported in an earlier paper [18] and this paper concentrates on the fragmentation of hybrid and complex glycans.

Materials and Methods

Materials

Hybrid and complex glycans were released with hydrazine [19, 20] from the well-characterized glycoproteins: porcine thyroglobulin [21, 22], chicken ovalbumin [23, 24], bovine fetuin [25], thyroglobulin and α1-acid glycoprotein [26]°obtained°from°Sigma°Chemical°Co.°Ltd. (Poole, Dorset, UK). Bi- and tri-antennary complex *N*-linked glycans were obtained as reference compounds from Oxford GlycoSciences Ltd., (Abingdon, UK) or were derived from the sialylated glycans by desialylation with 10% acetic acid for 30 min at 80 °C. Ammonium nitrate was from Aldrich Chemical Co. Ltd (Poole, UK). Methanol was obtained from BDH Ltd. (Poole, UK). Water was distilled before use.

Methylation of the Carboxy Group of Sialic Acids

In order to stabilize the sialic acids, the carboxy groups of°glycans°from°bovine°fetuin,°as°a°representative°example, were converted into their methyl esters by exchanging the protons for sodium and reacting the product with methyl iodide as described by Powell and Harvey°[27].

Published online March 11, 2005

Address reprint requests to Dr. D. J. Harvey, Department of Biochemistry, Glycobiology Institute, University of Oxford, South Parks Road, Oxford OX1 3QU, United Kingdom. E-mail: dh@glycob.ox.ac.uk

1044-0305/05/$30.00
doi:10.1016/j.jasms.2005.01.006

Received October 5, 2004
Revised January 5, 2005
Accepted January 5, 2005

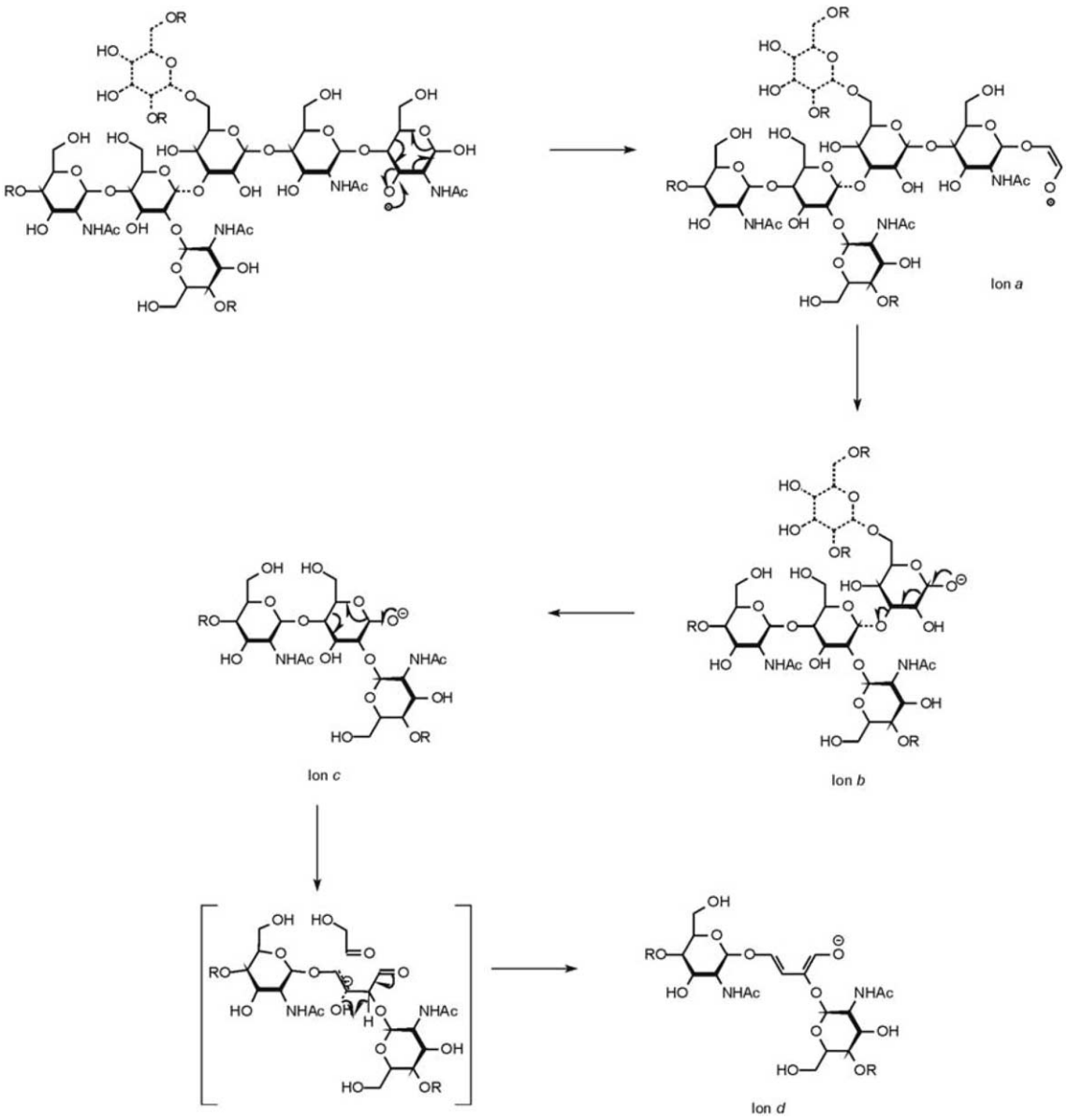

Scheme 1. Proposed mechanism for the formation of the ion E (Ion *d*).

Electrospray Mass Spectrometry

Electrospray ionization mass spectrometry was performed with a Waters-Micromass quadrupole-time-of-flight (Q-TOF) Ultima Global instrument (Waters/Micromass Ltd., Manchester, UK) as described earlier [17].

Investigations of the Effect of the RF-1 and Collision Cell Voltages

The carbohydrates, in solutions containing ammonium nitrate, were infused at 5 μL/min at a concentration of about 50 pmol total glycans/μL and spectra were recorded for 20 s with an acquisition time of 2 s (10 scans). For measurements of the effect of the RF-1 potential, this voltage was raised in 10 V steps from 0 to 250 V and spectra were recorded at each voltage. For measurements of the effect of collision cell potential, the RF-1 voltage was set at 250 and 80 V for the singly- and doubly-charged respectively and the collision cell potential was raised in 2 V steps from the voltage at which the fragments started to appear until most ions had fragmented.

Results and Discussion

Ion Nomenclature

Ion nomenclature follows that proposed by Domon and Costello [28] and as modified by Harvey et al. [18, 29] in order to accommodate changes in the glycan numbering as the result of differing antenna lengths. The numbering system for fragments retains that for the molecular ion.

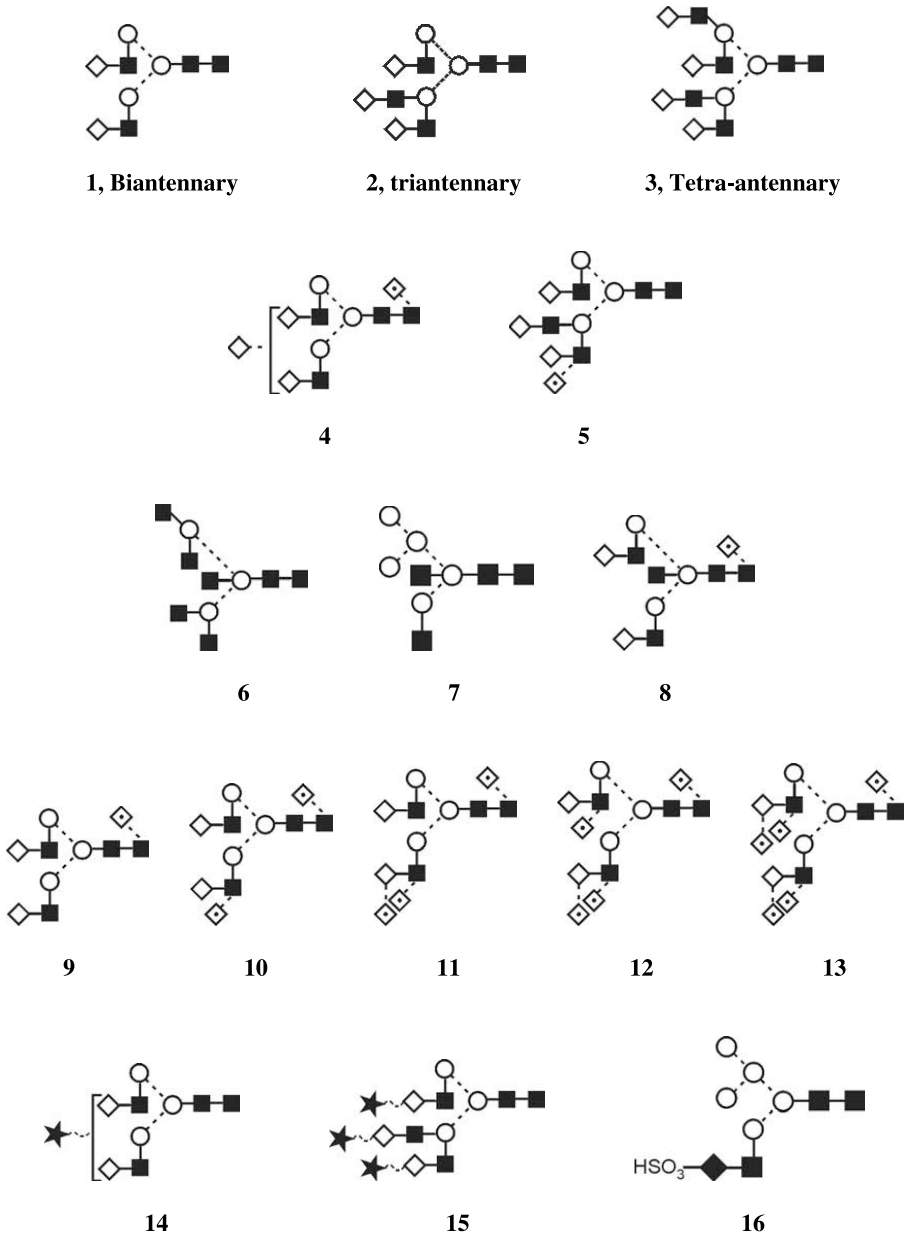

Figure 1. Structures of the glycans whose fragmentation is discussed in this paper. Key to symbols for this and subsequent figures: open circle = mannose, filled square = GlcNAc, open diamond = galactose, diamond with a dot in the center = fucose, filled star = *N*-acetylneuraminic (sialic) acid. The linkage position is shown by the angle of the lines linking the sugar residues (vertical line = 2-link, forward slash = 3-link, horizontal line = 4-link, back slash = 6-link). Full lines = β-bonds, broken lines = α-bonds. A wavy line linking the sialic acid residues indicates the presence of both $\alpha 2 \rightarrow 3$ and $\alpha 2 \rightarrow 6$ linkages.

Ions Produced by Fragmentation of the Chitobiose Core

Fragmentation of the chitobiose core of the hybrid and complex neutral glycans produced the same ions as noted earlier [18] for fragmentation of the high-mannose glycans. Thus, the most abundant ions were the $^{2,4}A_R$ (Ion *a*, Scheme **1**) and $^{2,4}A_{R-1}$ ions at $[M - HR - 161]^-$ and $[M - HR - 364]^-$ (where R is the attached anion) (Figures 2, 3b, 4a, 5a). When fucose was present at the 6-position of the reducing-terminal GlcNAc residue (Compounds **4**, **8**, **9–13**, Figure 1) (Figures 3a, 5b, 6), these ions appeared at $[M - HR - 307]^-$ and $[M - HR - 510]^-$ as the fucose was lost. For example, in the spectrum of the complex bi-antennary glycan, $(Gal)_2(Man)_3(GlcNAc)_4$ (**1**, Figure 2a), these two ions appeared at *m/z* 1478.6 ($^{2,4}A_R$) and 1275.5 ($^{2,4}A_{R-1}$), respectively. B-type fragments and the $^{O,2}A_R$ cross-ring fragment observed earlier were also present in all spectra. Mechanisms for the formation of these ions were proposed earlier [18].

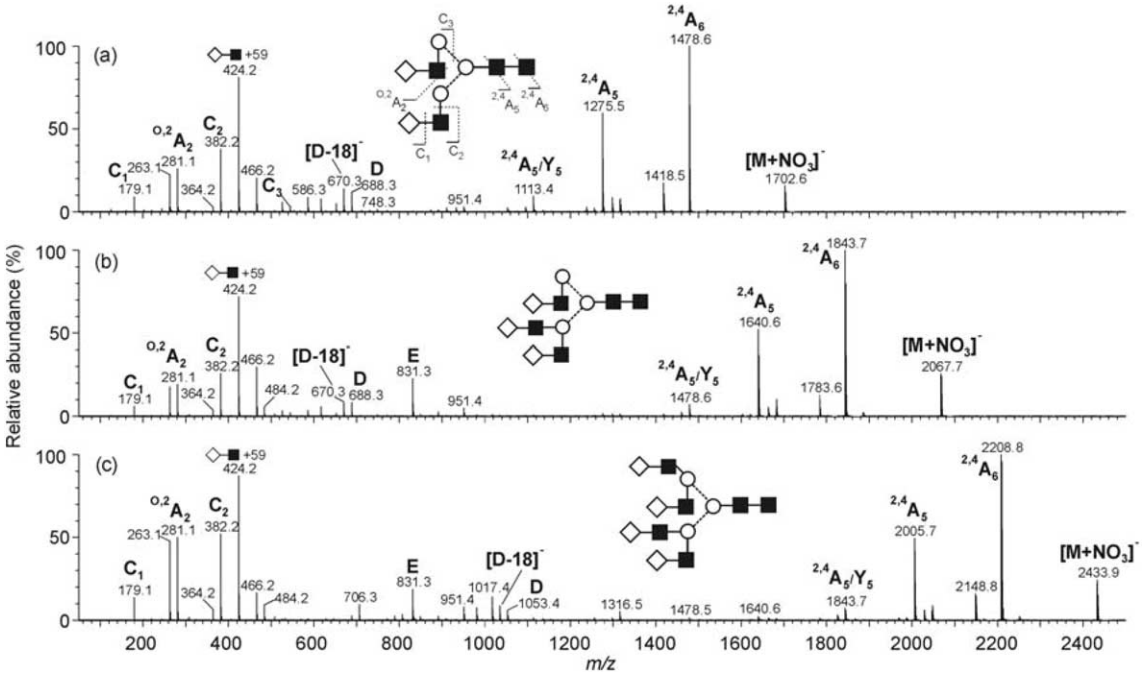

Figure 2. CID spectra of the $[M + NO_3]^-$ ions from the complex (**a**) bi- (**1**) (**b**), tri- (**2**), and (**c**) tetra-antennary (**3**) glycans.

Ions Specific to the 6-Antenna

The D (Ion e, Scheme **2**) and $[D - 18]^-$ ions reported earlier°[18]°as°being°diagnostic°for°the°composition°of the 6-antennas were prominent in the spectra of all glycans that did not contain a bisecting GlcNAc residue (see below). Thus, complex glycans containing a 6-antenna having the Gal → GlcNAc → Man chain (bi-antennary°[**1**,°Figure°2a]°and°3-branched°tri-antennary [**2**,°Figure°2b])°gave°*m/z* 688.3°and°670.3°whereas°tetra-antennary°(**3**,°Figure°2c)°and°6-branched°tri-antennary glycans gave spectra containing *m/z* 1053.4 and 1035.4.

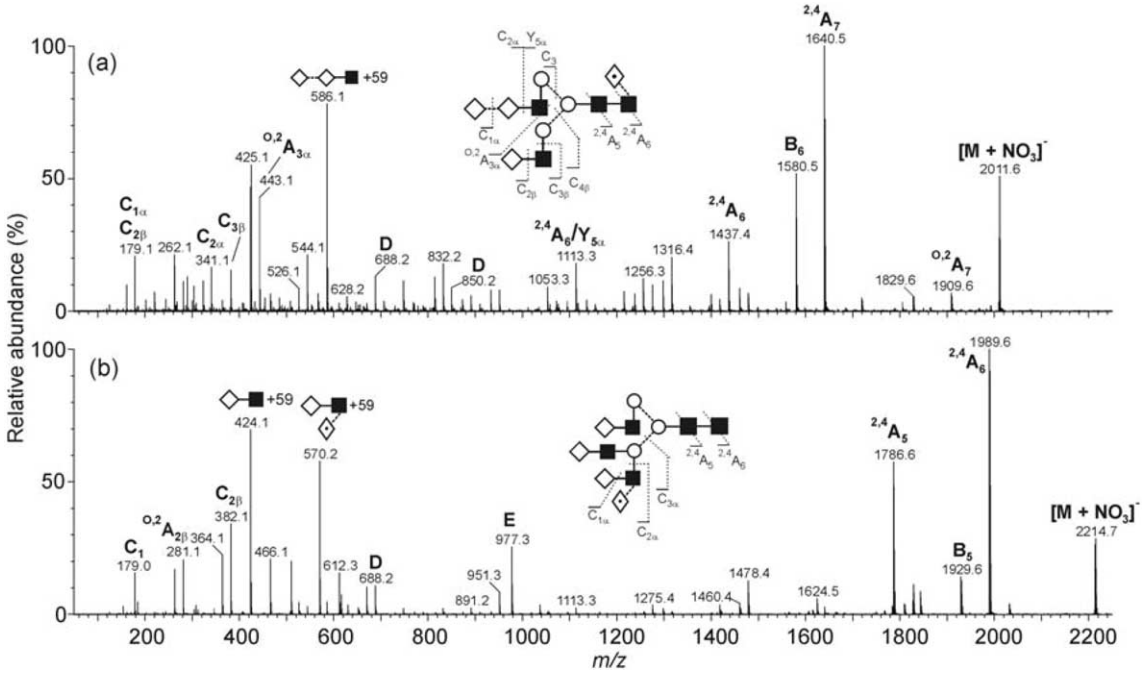

Figure 3. CID spectra of the $[M + NO_3]^-$ ion from (**a**) the α-galactosylated bi-antennary glycan (**4**) from porcine thyroglobulin and (**b**) the monofucosylated tri-antennary glycan (**5**) from human α1-acid glycoprotein.

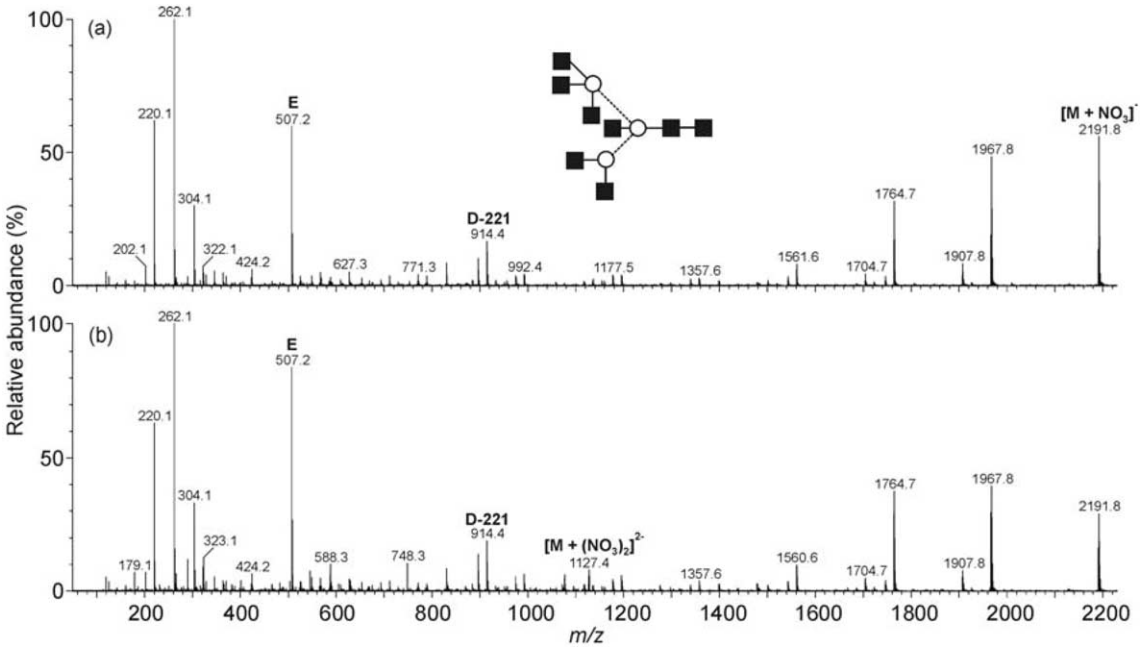

Figure 4. CID spectrum of (**a**) the $[M + NO_3]^-$ ion and (**b**) the $[M + (NO_3)_2]^{2-}$ ion from the complex penta-antennary glycan (**6**) from chicken egg-white glycoproteins.

The presence of an α-galactose residue on both the 3- and 6-antenna of one of the glycans from porcine thyroglobulin (Compound **4**) was demonstrated by the presence of the D and $[D - 18]^-$ ions at *m/z* 688.2, 770.2, and at *m/z* 850.3, 832.3, respectively (Figure 3a). Previous reports [21] had suggested that only the 6-antenna was substituted with an α-galactose residue but the complexity of the spectrum clearly shows that it is from a mixture. Table 1 lists the masses of Ion D found in the spectra of common *N*-linked glycans. The D ion appears to be formed by a C_{R-1}/Z° cleavage [18] unlike its formation in positive ion spectra where a B/Y cleavage appears to be involved [29]. $^{O,3}A_4$ cross-ring cleavages (e.g., *m/z* 616.3, Figure 2a) also produced abundant ions in these spectra that specified the composition of the 6-antenna.

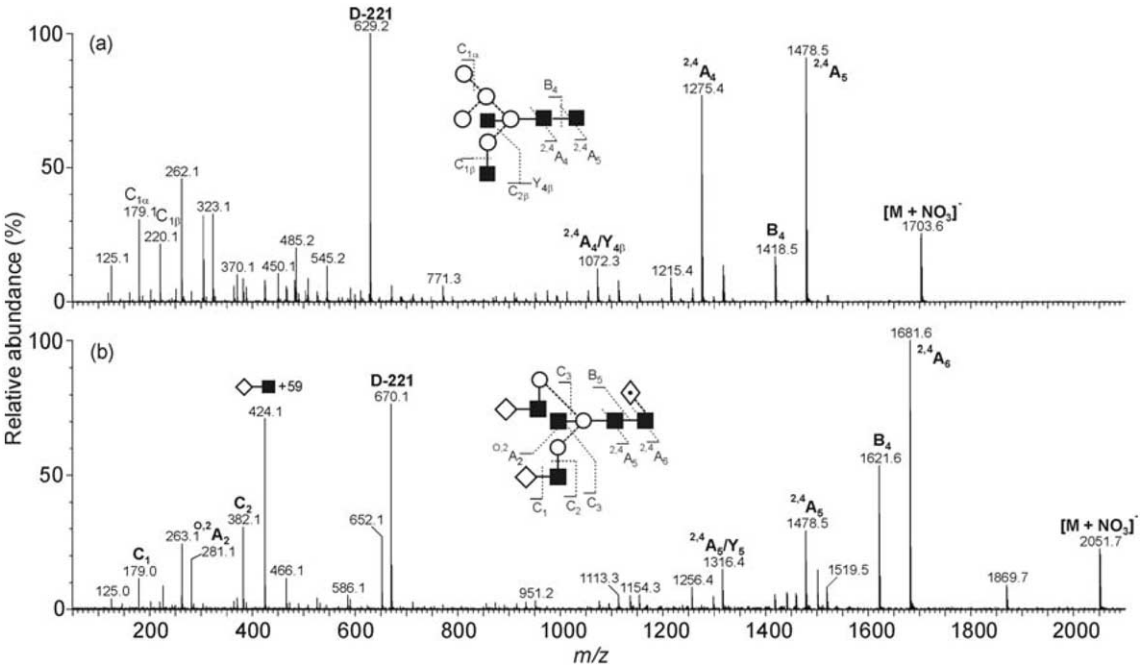

Figure 5. CID spectrum of the $[M + NO_3]^-$ ion from (**a**) the hybrid glycan (**7**) from chicken ovalbumin and (**b**) the bisected bi-antennary glycan (**8**).

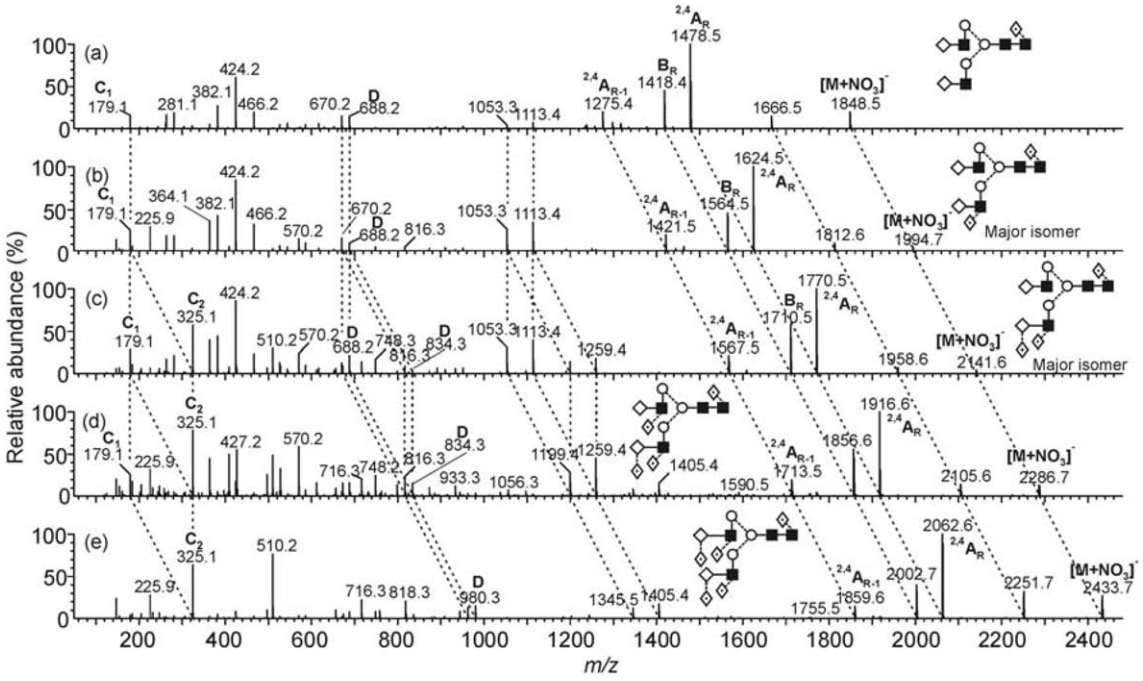

Figure 6. CID spectra of the $[M + NO_3]^-$ ions from bi-antennary glycans carrying from one to five fucose residues (**9**–**13**). Broken lines connect ions of the same type.

Prominent A-type cross-ring cleavage ions were formed by cleavage of the mannose residues attached to the GlcNAc residues of the antennas following charge localization on an oxygen atom adjacent to the site of attachment of the GlcNAc such that two carbon atoms from the mannose residue remained in the ion. Thus, the spectra of complex glycans containing Gal → GlcNAc antennas exhibited a prominent fragment at *m/z* 424.1 (Figures 2–4) corresponding to $[Gal\text{-}GlcNAc + 59]^-$ ($^{1,3}A_3$ fragment). Substitution by α-galactose, as in the glycan from porcine thyroglobulin (**4**, Figure 3a) caused a shift of 162 u to *m/z* 586.1 whereas fucose substitution (**5**, Figure 3b) produced a shift to *m/z* 570.2. The latter ion demonstrates the stability of fucose in these negative ion spectra in direct contrast to its instability in the spectra of $[M + Na]^+$ ions [30]. Where no galactose residue capped the antennas, as in glycans from chicken egg-white glycoproteins (**8**, Figure 4a), this A-type ion appeared at *m/z* 262.1. Unlike the situation with several of the other fragment ions, this ion was observed from all antennas, irrespective of the linkage of the GlcNAc residue to the mannose.

Ions Providing Information on the 3-Antenna

Unlike the spectra of the high-mannose glycans, where the composition of the 3-antenna was determined by subtraction of the masses of the 6-antenna (defined by the D, [D − 18]- and $^{O,3}A_3$ ions), an ion providing information on the 3-antenna was present in the spectra of the complex and hybrid glycans. This ion appeared at *m/z* 466.2 in the spectra of the bi-antennary glycans and contained the galactose and GlcNAc residues plus 101 mass units from the 3-mannose residue. In the spectra of the tri-antennary glycans from bovine fetuin, containing a branched 3-antenna, this ion partially shifted to *m/z* 813.3 (**2**, Figure 2b) showing that it contained C2 and C4 from the mannose residue. Consequently, it must also contain C3 together with a fourth carbon atom. Ions of this type will be referred to as E-type ions. The ion was prominent in the spectra of the truncated (no galactose) complex and hybrid glycans from hen egg white glycoproteins, (*m/z* 304 when one GlcNAc residue was present (**7**, Figure 5a) and *m/z* 507 when there were two, (**6**, Figure 4a, Table 2) confirming its composition. The structure of this ion appears to be as shown in Scheme **1** (Ion *d*) and a possible mechanism is proposed following formation of a second C-cleavage ion from the C_3-ion (Ion *c*). The fragmentation of this second C-cleavage ion differs from that of the decomposition of Ion *b* shown in the earlier paper [18] because the oxygen at C-2 carries a sugar residue rather than a hydrogen atom. As noted above, Ion E (Structure *d*) was prominent at *m/z* 831.3 in the spectrum of the tri-antennary glycan from bovine fetuin (**2**, Figure 2b, branched 3-antenna). In the spectrum of the fucosylated tri-antennary glycan from α1-acid glycoprotein (**5**, Figure 3b) which also has a branched 3-antenna, known to contain an unusual fucose substitution in an antenna rather than on the core GlcNAc [26], the presence of a prominent ion at *m/z* 977.4 and the absence of *m/z* 831.3 confirmed the presence of the fucose on the 3- rather than on the 6-antenna.

Although the mass of ion E reflects the composition of the 3-antenna, the spectra of the tri-antennary (Figure

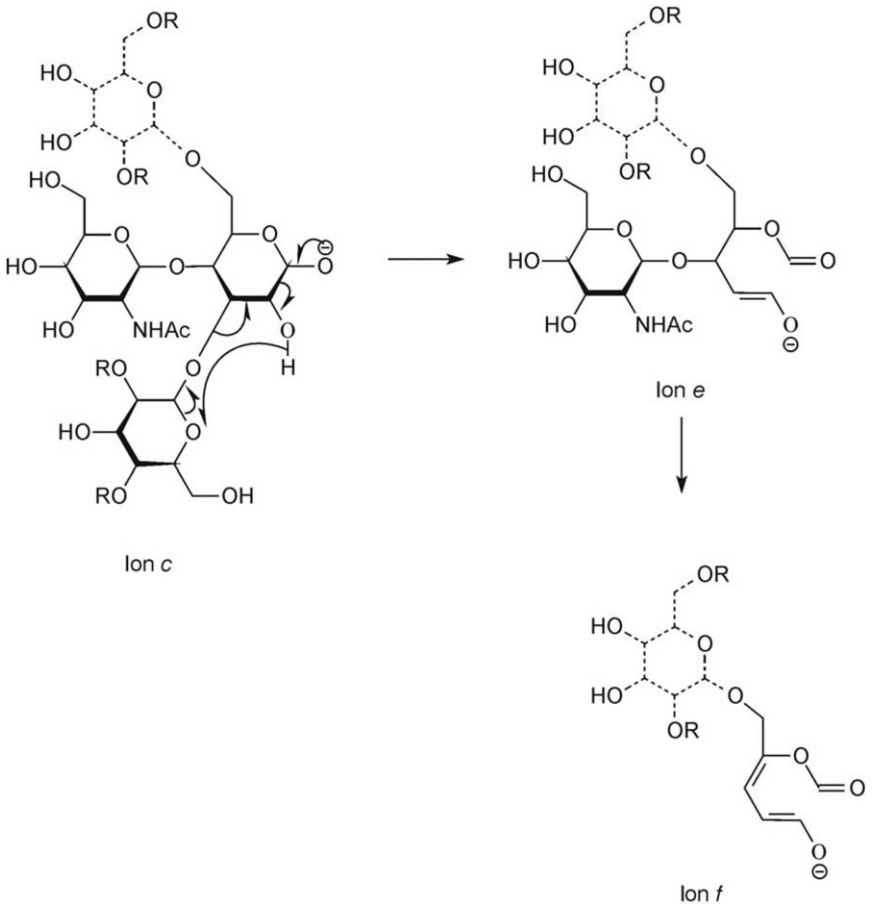

Scheme 2. Proposed mechanism for the formation of the ion diagnostic for the presence of a bisecting GlcNAc residue. The source of the hydrogen eliminated during loss of the bisecting GlcNAc residue has not been confirmed.

2b)°and°tetra-antennary°glycans°(Figure°2c)°also°contained an ion at *m/z* 466.2, the mass of ion E in the spectrum°of°the°bi-antennary°glycan°(Figure°2a).°This ion appears to arise from the 6-antenna and is a consequence of this antenna containing a similar substitution pattern to the bi-antennary glycan, namely a 2-linked GlcNAc residue, thus accounting for its presence° in° the° spectra° of° the° bi-° (Figure° 2a)° and° triantennary° (Figure° 2b)° glycans.° However,° the° tetra-antennary glycan also contains an ion at this mass. This mass is a consequence of the tetra-antennary containing its second branch at the 6- rather than the 4-position. As discussed above, Ion E contains only carbon atoms 1–4 from the mannose residue and, consequently, Ion

Table 1. Masses and compositions of the D-ion specifying the composition of the 6-antenna of *N*-linked glycans

m/z, D ion	*m/z* D-18	Hexose	HexNAc	Type of glycan
323	305	1	0	Unprocessed 6-antenna (e.g. $(Man)_3(GlcNAc)_2$).
485	467	2	0	High-mannose, Hybrid.
526	508	1	1	Truncated (no galactose), unbranched 6-antenna.
647	629	3	0	High-mannose, Hybrid.
688	670	2	1	Biantennary, 3-branched triantennary.
729	711	1	2	Truncated (no galactose), branched 6-antenna.
809	791	4	0	High-mannose, Hybrid (e.g. $(Man)_5(GlcNAc)_2$).
891	873	2	2	Triantennary (branched 6-antenna), one galactose.
932	914	1	3	Truncated (no galactose), branched 6-antenna with bisected mannose.
1053	1035	3	2	Triantennary (branched 6-antenna).
1094	1076	2	3	Branched 6-antenna with bisected mannose and one galactose.

Table 2. Masses and compositions of Ion E

m/z	Hexose	HexNAc	dHex
304	1	1	0
466	2	1	0
507	1	2	0
669	2	2	0
831	3	2	0
977	3	2	1

E from the 6-antenna contains only the 2-branch and appears at *m/z* 466.2. Differentiation of ion E from each antenna (termed E_3 and E_6 from the 3- and 6-antennas, respectively) can be made on the basis of the known structure of the 6-antenna as determined by the masses of the D and $^{O,3}A_4$ cross-ring cleavage ions. Furthermore, the mass of ion E_6 can be used to define the substitution on each branch of the 6-antenna as it only contains the 2-branch.

Ions Revealing Antenna Sequence

C-ions derived from the non-reducing terminus provided information on antenna sequence, as illustrated for the bi-antennary glycan (**1**, Figure 2a) which contained C ions at *m/z* 179.1 (Gal, C_1), 382.2 (Gal → GlcNAc, C_2) and 544.3 (Gal → GlcNAc → Man, C_3). However, in order to observe the other C-ions, the collision energy had to be reduced in order to avoid their further decomposition. Nevertheless, they were present at low abundance as described earlier [18]. Where antennas of unequal composition were present, C ions enabled the sequence of both antennas to be traced as shown in Figure 3.

The 1 → 4-linkage between the galactose and GlcNAc residues of the antennas of complex glycans was reflected by an $^{O,2}A_2$ cross-ring cleavage of the GlcNAc residue to give the ion at *m/z* 281.1 (Figure 2, mechanism as in the formation of Ion a, Scheme **1**). It partially shifted to *m/z* 443 when an α-galactose residue was present (**4**, Figure 3a). Ions were not found that allowed the α-Gal → β-Gal linkage to be determined.

Ions Diagnostic for the Presence of a Bisecting GlcNAc Residue

Figure 5a shows the spectrum of the $[M + NO_3]^-$ ion from the hybrid glycan $(Man)_5(GlcNAc)_4$ (**7**) from chicken ovalbumin which was dominated by the ion at *m/z* 629.2. Corresponding ions were present at *m/z* 670.2 and 914.4 in the spectra of the nitrate adducts of the bisected bi-antennary glycan (**8**, Figure 5b) and penta-antennary glycan (**6**, Figure 4a). This ion equates to that formed by loss of water from the D-ion in the spectra of unbisected glycans. In the high-energy positive ion spectra of $[M + Na]^+$ ions, the equivalent $[D - GlcNAc]^-$ ion has been shown to be diagnostic for the presence of a bisecting GlcNAc residue and to be formed by loss of the bisecting GlcNAc from the B_{R-1} ion followed by a Y-type loss of the 3-antenna [29]. However, the mechanism in these negative ion spectra appears to be that shown in Scheme **2** to give the D-ion (Ion *e*) followed by elimination of the allylic GlcNAc residue together with a hydrogen atom from an undetermined position. The D ion itself (Ion *e*) was very weak in these spectra (*m/z* 850.3 in Figure 5a) reflecting the ready elimination of the GlcNAc residue. Thus, the absence of, or presence of a very weak D ion accompanied by a very strong $[D - (GlcNAc + H_2O)]^-$ ion indicates the presence of a bisecting GlcNAc residue. This feature is difficult to determine by exoglycosidase digestion because of the absence of a specific exoglycosidase for a bisecting GlcNAc residue.

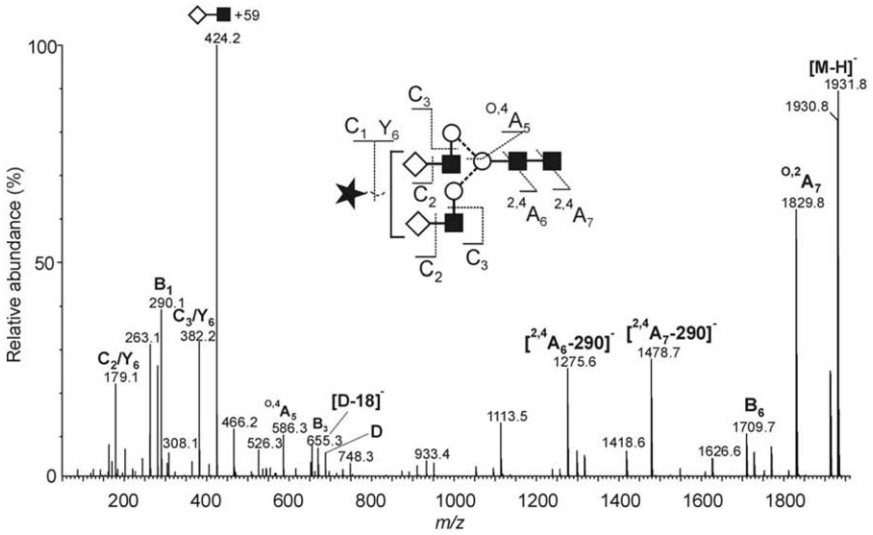

Figure 7. CID spectrum of the $[M - H]^-$ ion from the monosialylated complex bi-antennary glycan (**14**) from bovine fetuin. Because the antenna to which the sialic acid is linked is not known, both antennas are numbered as if the sialic acid was present.

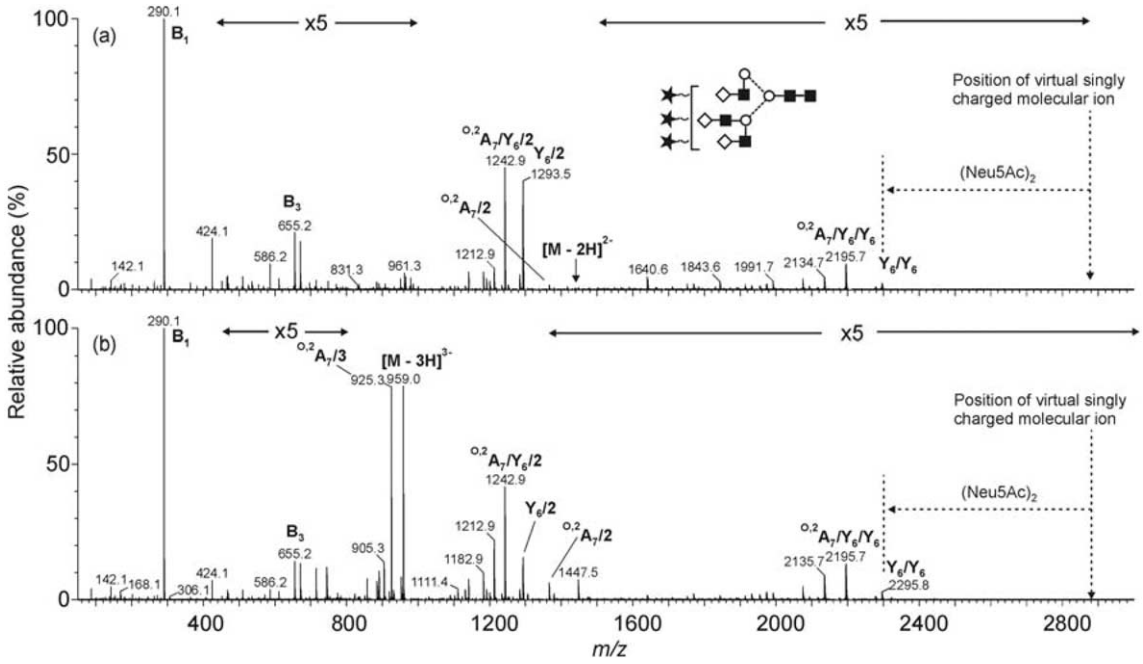

Figure 8. CID spectra of the doubly-charged ($[M - 2H]^{2-}$) (**a**) and triply-charged ($[M - 3H]^{3-}$) (**b**) ions from the sialylated tri-antennary glycan (**15**) from bovine fetuin.

Ions Diagnostic for the Position of Fucose Substitution

Unlike the situation with positive ion spectra, the antenna-specific ions discussed above largely retained fucose allowing substitution patterns to be determined. Figure 6 shows the spectra of the bi-antennary *N*-linked glycan $(Gal)_2(Man)_3(GlcNAc)_4$, (**2**) obtained from human parotid glands substituted with from one to five fucose residues (Compounds **9**–**13**). Their structures have been described earlier [30, 31]. The spectra of the mono- (**9**) and penta-fucosylated compounds (**13**) are from single compounds but the remaining spectra are from mixtures of isomers.

The mono-fucosylated glycan (**9**, Figure 6a) contains its fucose on the 6-position of the reducing terminal GlcNAc residue giving the prominent losses of 370 ($^{2,4}A_R$, *m/z* 1478.5), 573 ($^{2,4}A_{R-1}$, *m/z* 1275.4), and 430 (B_R, *m/z* 1418.3) mass units in the spectra of the nitrate adduct, as discussed above. In the spectra of the other glycans, shifts of the D and $[D - 18]^-$ ions were the most diagnostic of the position of fucose substitution. Thus, in the spectra of the di-fucosylated glycan (**10**, Figure 6b) these ions remained largely unshifted with only a small fraction exhibiting a shift from *m/z* 688.2/670.2 to 834.3/816.3, showing that the major isomer was substituted on the 3-antenna. The observation that the C_1 (galactose) ion at *m/z* 179.1 exhibited no shift showed that the fucose was substituted on the GlcNAc residue. The trifucosylated glycan (**11**, Figure 6c) also exhibited little shift in the D and $[D - 18]^-$ ions consistent with the reported major structure that has a core fucose and two fucose residues on the 3-antenna [31]. The appearance of an abundant C_1 ion at *m/z* 325.1 confirmed substitution of the third fucose residue on the galactose. In the spectrum of the tetrafucosylated glycan (**12**, Figure 6d), the C_2 ion appeared at *m/z* 528.2 and 674.2, corresponding to antennas containing one and two fucose residues respectively. However, there was an abundant $[C_2 - 164]^-$ ion (*m/z* 364.2) corresponding to the $[C_2 - H_2O]^-$ ion in the spectrum of the unfucosylated glycan and, therefore, formed by loss of a fucose molecule. As substituents linked to the 3-position of GlcNAc are known to be preferentially eliminated [32–36], this observation can be used to demonstrate the presence of a fucose residue in this position. The $[C_2 -$ fucose$]^-$ ion appeared at *m/z* 510.2.1 in the spectrum of the pentafucosylated glycan (**13**, Figure 6e) as this

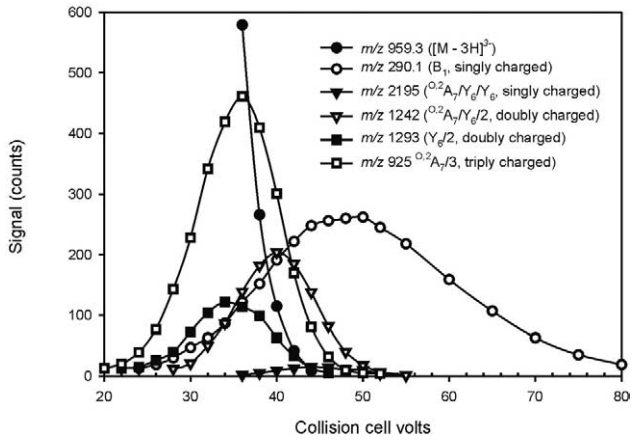

Figure 9. Energy-resolved spectrum for the $[M - 3H]^{3-}$ ion from the trisialylated tri-antennary glycan (**15**) from bovine fetuin.

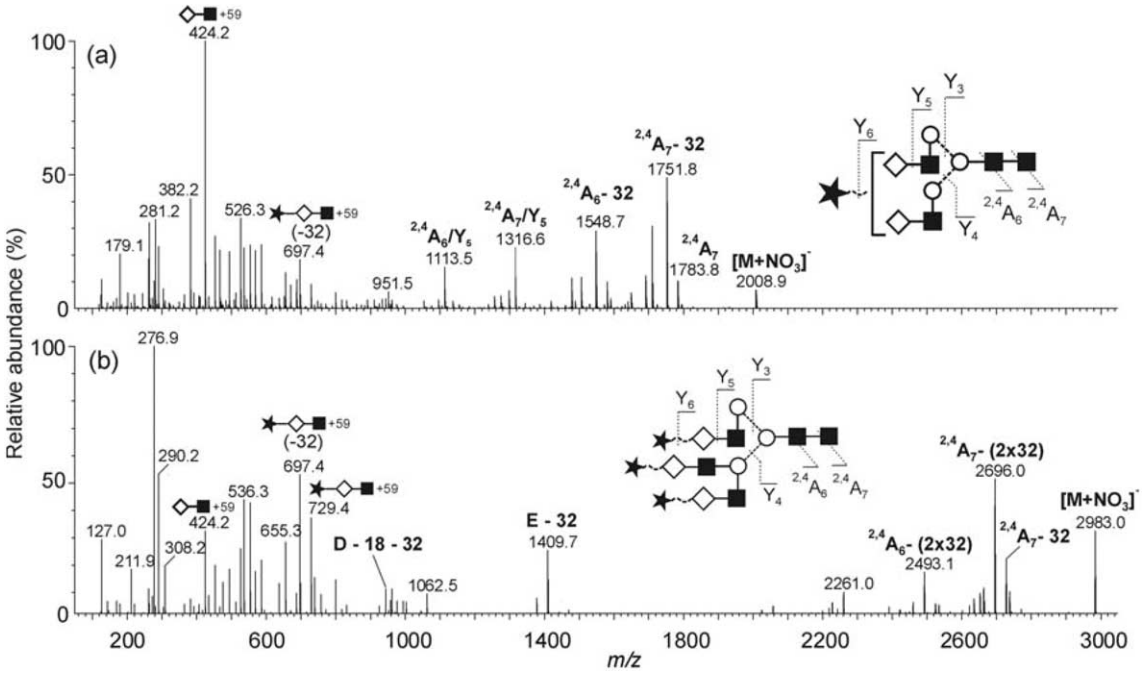

Figure 10. CID spectrum of the nitrate adducts of the methyl esters of (**a**) the monosialylated bi-antennary glycan (**14**) and (**b**) the disialylated tri-antennary glycan.

compound contained two antennas substituted with fucose at the 3-position of GlcNAc.

Ions corresponding to loss of Gal → GlcNAc from the $[M - H - 161]^-$ and B_R ions of the nitrate adducts also reflected the distribution of the fucose residue on the antennas. Thus, in the spectrum of the difucosylated glycan (**10**, Figure 6b), shown to be fucosylated mainly on the 3-antenna, these ions largely remained at *m/z* 1113.3 and 1053.3, respectively showing that they were products of the loss of the 3- rather than the 6-antenna. Their shifts and relative abundance in the other three spectra (Figure 6c–e) paralleled that of the D and $[D - 18]^-$ ions, and are, therefore, also indicative of the substitution pattern of the fucose residues. The mechanisms forming these ions are unclear as they appear to involve loss of the reducing-terminal GlcNAc residue (B_R ion) or a fragment of it ($^{2,4}A_R$ ion) together with a specific loss of the 3-antenna. Electron shifts through the sugar rings linking these sites are not possible without initiating glycosidic cleavages and, therefore, the presence of these specific cleavages suggests the occurrence of a specific hydrogen transfer to either the fragment formed at the reducing terminal from the 3-antenna or vice versa in a similar manner to the proposed losses of mannose residues from the $^{2,4}A_{R-1}$ ion discussed in reference [18].

Fragmentation of Doubly-Charged Ions from Neutral Glycans

The $[M + (NO_3)_2]^{2+}$ ions from the complex and hybrid glycans fragmented exclusively to singly-charged fragments that mirrored the fragment ions seen in the spectra of the singly-charged $[M + NO_3]^-$ ions as shown for the truncated penta-antennary glycan **6** (Figure 4). Thus, because there was sometimes a tendency for the larger glycans to form doubly-charged ions in preference to singly-charged ions, the singly-charged fragmentation spectrum could easily be obtained.

Fragmentation of Sialylated Glycans

Underivatized glycans. The monosialylated complex glycans fragmented in a similar manner to the neutral compounds in that they produced the same C, D, and E ions and a prominent ion corresponding to [Gal → GlcNAc + 59]$^-$ ($[^{1,3}A_3 - Neu5Ac]^-$, *m/z* 424.2) as exemplified by the spectrum of the monosialylated bi-antennary glycan (**14**, Figure 7). However, the upper mass region was different. The ion formed by loss of 161 mass units (*m/z* 1769.7, $^{2,4}A_R$), prominent in the spectra of the neutral glycans, was weak due to a further loss of sialic acid which gave the ion at *m/z* 1478.5 ($^{2,4}A_R/Y_{NR}$). Similarly the $^{2,4}A_{R-1}$ ion was replaced by a $^{2,4}A_{R-1}/Y_{NR}$ fragment at *m/z* 1275.5). There was a weak B_R ion (*m/z* 1709.6) but an abundant ion formed by loss of 101 mass units (HO-CH=CH-NHAc, $^{O,2}A_R$ or possibly a $^{3,5}X_{NR}$ cleavage). A B_{NR} cleavage gave the sialic acid residue ion at *m/z* 290.1.

Figure 8 shows the CID spectra of the doubly- and triply-charged ions from the trisialylated tri-antennary glycan (**15**), and Figure 9 shows how the abundance of the fragment ions varied with collision cell energy. The doubly-charged ion (*m/z* 1438.5, Figure 8a) showed a pattern of doubly-charged fragments that mirrored the upper mass range of the singly-charged ion from the

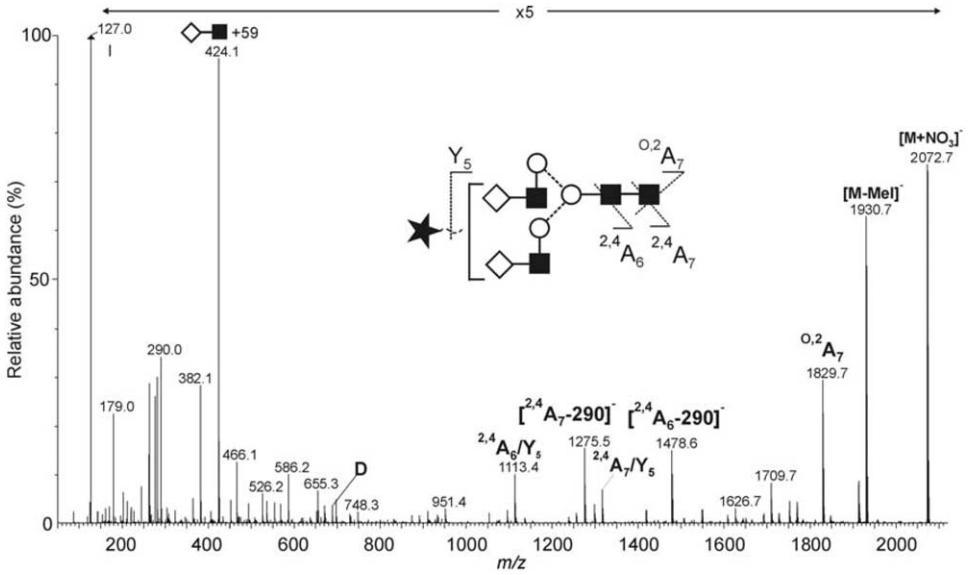

Figure 11. CID spectrum of the iodide adduct of the methyl ester of the monosialylated bi-antennary glycan (**14**).

monosialylated glycan, namely $^{O,2}A_R$ and $^{2,4}A_R$ cleavages and losses from them of a further sialic acid residue (Y-cleavage). Singly-charged fragments were formed by loss of a sialic acid residue with its charge and reflected the pattern of singly-charged ions from the $[M - H]^-$ ion. An abundant D-fragment at *m/z* 961.4 reflected the sialylated 6-antenna but the sialylated ion from the 3-antenna (E-type fragment), expected at *m/z* 1413, was missing. However, their desialylated counterparts were present at *m/z* 831 and 446 (Tables 1 and 2).

The triply-charged ion from the trisialylated, tri-antennary glycan from bovine fetuin (*m/z* 958.7, **15**, Figure 8b) gave a spectrum that was almost identical to that reported by Sagi et al. [16] from erythropoietin even though it was branched on the 3-linked antenna, whereas the reported spectrum came from a tri-antennary glycan that was branched on the 6-antenna. The most abundant ions were formed by the above reducing-end fragments as singly-, doubly- and triply-charged fragments, the singly- and doubly-charged fragments were the result of loss of two sialic acid residues with two and one charge, respectively. Although the arm-specific fragment ions were very weak or missing, a prominent singly-charged B_3 (B_{NR-2}) fragment at *m/z* 655 ([Neu5Ac-Gal-GlcNAc − H]$^-$) reflected the composition of the sialylated antennas. A similar spectrum was recorded from the disialylated bi-antennary glycan but with the addition of a prominent singly-charged C_4 ion at *m/z* 835. The corresponding ion was absent from the spectrum of the monosialylated glycan (singly-charged).

The linkage of the sialic acids could sometimes be determined from the presence or absence of several of the singly-charged ions as described in our earlier publication [10]. Thus, the presence of an ion at *m/z* 306.1 ($^{O,4}A_2$ - CO_2) indicated an $\alpha 2 \rightarrow 6$-linked sialic acid. Its relatively low abundance in the spectra of the sialylated glycans from bovine fetuin (Figures 7 and 8), compared with its abundance in the reported spectrum of the synthetic bi-antennary glycan with two $\alpha 2 \rightarrow 6$-linked sialic acid residues [10] suggested that both $\alpha 2 \rightarrow 3$- and $\alpha 2 \rightarrow 6$-linked sialic acids were present. This conclusion was supported by the ions at *m/z* 655.2 (B_3) and 671.2, whose relative abundance also appears to be a function of the sialic acid linkage.

Methyl Esters

Formation of the methyl esters of the sialic acids by the method described by Powell and Harvey [27] produced spectra similar to those of the neutral glycans because the charge again resided on hydroxy rather than acid groups. However, the spectra were complicated by ready losses of methanol from many of the diagnostic fragment ions that contained the derivatized sialic acid (Figure 10). Thus, for example, in the spectrum of the monosialylated bi-antennary glycan, the $^{2,4}A_R$, $^{2,4}A_{R-1}$, B_R, $^{2,4}A_R/Y_6$, $^{2,4}A_{R-1}/Y_6$, and $[D - 18]^-$ ions were largely replaced by their analogues that had lost methanol (Figure 10a). The spectrum of the nitrate analogue of the methylated disialylated tri-antennary glycan shown in Figure 10b shows losses of one and two molecules of methanol from these ions. The E-type ions defining the location of one and two sialic acid residues show losses of one methanol molecule for the ion containing one sialic acid residue (*m/z* 1136.5 and 1104.5) and both one (*m/z* 1409.7) and two (*m/z* 1377.6) molecules for the disialylated analogue.

The MS^1 spectrum of the methyl esters contained abundant $[M + I]^-$ ions as the result of the presence of

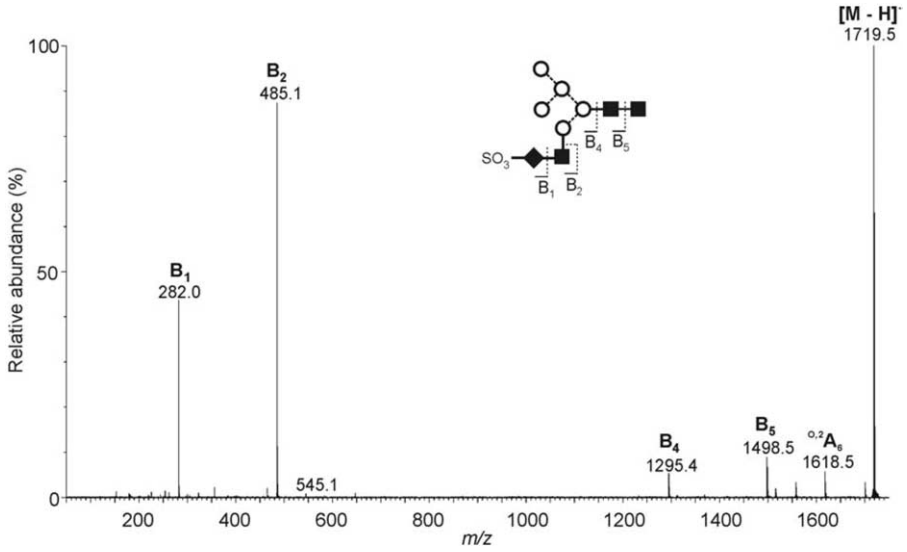

Figure 12. CID spectrum of the sulfated hybrid glycan (**16**) from equine luteinizing hormone.

residual iodine from the reaction with methyl iodide. These adducts showed weak fragmentation as described for the neutral glycans in the earlier paper [17] but with some differences from that of the nitrate adducts. Ions in the high-mass region were dominated by the loss of MeI to give the equivalent of the $[M - H]^-$ ion which then fragmented in a similar manner to the $[M - H]^-$ ions from the underivatized glycans (Figure 11).

Fragmentation of Sulfated Glycans

Sulfated glycans showed a different fragmentation pattern as illustrated by the spectrum of the $[M - H]^-$ ion from the hybrid glycan (**16**, Figure 12). Charge retention on the sulfate group gave abundant B_{NR} and B_{NR-1} cleavages adjacent to the two HexNAc residues of the 3-antenna to produce the major ions at *m/z* 282.0 and 485.0. The only other significant ions were $^{0,2}A_R$ (*m/z* 1618.5), $^{2,4}A_R$ (*m/z* 1558.5), B_R (*m/z* 1498.5), and B_{R-1} (*m/z* 1295.4).

Summary and Conclusions

Fragmentation of the hybrid and complex glycans followed the same general pattern as fragmentation of the high-mannose glycans; formation of most ions could be rationalized by initial abstraction of a proton from one specific hydroxy group. C-type glycosidic and cross-ring fragments dominated the spectra with $^{2,4}A_R$ and $^{2,4}A_{R-1}$ ions defining the structure of the fucosylated and non-fucosylated core. The stability of most cross-ring fragments appeared to be the result of the formation of an ionized enol structure. Formation of a C_{R-2} ion appeared to be a prerequisite to production of many of the other fragment ions.

Additional specific information that was revealed by these negative ion spectra included the sequence of the antennas (C-fragments), the composition of the individual antennas (D and E fragments from the 6-, and both 6 and 3-antennas, respectively, and $^{0,3}A$ fragment of the branching mannose residue), the presence or absence of a bisecting GlcNAc residue ($[D - 221]^-$ ion) and the position of substituents such of fucose on the antennas. These ions were the result of the more specific nature of the fragmentation of the negative ions compared with that of the corresponding positive ions and provided specific structural information that was not extractable from the positive ion spectra or from classical experiments involving exoglycosidase digestions.

Acknowledgments

The author thanks Professor R. A. Dwek, Director of the Glycobiology Institute, for his help and encouragement and Dr. George R. Bousfield for permission to include the result from the sulfated glycan. The author is grateful to one of the reviewers who pointed out that ion E could arise from the 6- as well as the 3-antenna. He also thanks the Wellcome Trust for an equipment grant to purchase the Q-TOF mass spectrometer.

References

1. Varki, A. Biological roles of oligosaccharides: All of the theories are correct. *Glycobiology* **1993,** *3,* 97–130.
2. Dwek, R. A. Glycobiology: Towards understanding the function of sugars. *Chem. Rev.* **1996,** *96,* 683–720.
3. Dwek, R. A.; Edge, C. J.; Harvey, D. J.; Wormald, M. R.; Parekh, R. B. Analysis of glycoprotein-associated oligosaccharides. *Ann. Rev. Biochem.* **1993,** *62,* 65–100.
4. Rudd, P. M.; Dwek, R. A. Rapid, sensitive sequencing of oligosaccharides from glycoproteins. *Curr. Opin. Biotechnol.* **1997,** *8,* 488–497.
5. Rudd, P. M.; Guile, G. R.; Küster, B.; Harvey, D. J.; Opdenakker, G.; Dwek, R. A. Oligosaccharide sequencing technology. *Nature* **1997,** *388,* 205–207.
6. Rudd, P. M.; Colominas, C.; Royle, L.; Murphy, N.; Hart, E.; Merry, A. H.; Hebestreit, H. F.; Dwek, R. A. A high-perfor-

mance liquid chromatography based strategy for rapid, sensitive sequencing of N-linked oligosaccharide modifications to proteins in sodium dodecyl sulphate polyacrylamide electrophoresis gel bands. *Proteomics* **2001,** *1,* 285–294.
7. Sutton, C. W.; O'Neill, J. A.; Cottrell, J. S. Site-specific characterization of glycoprotein carbohydrates by exoglycosidase digestion and laser desorption mass spectrometry. *Anal. Biochem.* **1994,** *218,* 34–46.
8. Harvey, D. J.; Rudd, P. M.; Bateman, R. H.; Bordoli, R. S.; Howes, K.; Hoyes, J. B.; Vickers, R. G. Examination of complex oligosaccharides by matrix-assisted laser desorption/ionization mass spectrometry on time-of-flight and magnetic sector instruments. *Org. Mass Spectrom.* **1994,** *29,* 753–765.
9. Zaia, J. Mass spectrometry of oligosaccharides. *Mass Spectrom. Rev.* **2004,** *23,* 161–227.
10. Wheeler, S. F.; Harvey, D. J. Negative ion mass spectrometry of sialylated carbohydrates: Discrimination of *N*-acetylneuraminic acid linkages by matrix-assisted laser desorption/ionization-time-of-flight and electrospray-time-of-flight mass spectrometry. *Anal. Chem.* **2000,** *72,* 5027–5039.
11. Chai, W.; Piskarev, V.; Lawson, A. M. Negative-ion electrospray mass spectrometry of neutral underivatized oligosaccharides. *Anal. Chem.* **2001,** *73,* 651–657.
12. Pfenninger, A.; Karas, M.; Finke, B.; Stahl, B. Structural analysis of underivatized neutral human milk oligosaccharides in the negative ion mode by nano-electrospray MS^n; Part 1. Methodology. *J. Am. Soc. Mass Spectrom.* **2002,** *13,* 1331–1340.
13. Pfenninger, A.; Karas, M.; Finke, B.; Stahl, B. Structural analysis of underivatized neutral human milk oligosaccharides in the negative ion mode by nano-electrospray MS^n; Part 2. Application to isomeric mixtures. *J. Am. Soc. Mass Spectrom.* **2002,** *13,* 1341–1348.
14. Chai, W.; Piskarev, V.; Lawson, A. M. Branching pattern and sequence analysis of underivatized oligosaccharides by combined MS/MS of singly and doubly charged molecular ions in negative-ion electrospray mass spectrometry. *J. Am. Soc. Mass Spectrom.* **2002,** *13,* 670–679.
15. Quéméner, B.; Désiré, C.; Lahaye, M.; Debrauwer, L.; Negroni, L. Structural characterization of both positive- and negative-ion electrospray mass spectrometry of partially methyl-esterified oligogalacturonides purified by semi-preparative high-performance anion-exchange chromatography. *Eur. J. Mass. Spectrom.* **2003**, *9,* 45–60.
16. Sagi, D.; Peter-Katalinic, J.; Conradt, H. S.; Nimtz, M. Sequencing of tri- and tetra-antennary N-glycans containing sialic acid by negative mode ESI QTOF tandem MS. *J. Am. Soc. Mass Spectrom.* **2002,** *13,* 1138–1148.
17. Harvey, D. J. Fragmentation of negative ions from carbohydrates; Part 1. Use of nitrate and other anionic adducts for the production of negative ion electrospray spectra from *N*-linked carbohydrates. *J. Am. Soc. Mass Spectrom.* **2005,** *16*, 622–630.
18. Harvey, D. J. Fragmentation of negative ions from carbohydrates; Part 2. Fragmentation of high-mannose *N*-linked glycans. *J. Am. Soc. Mass Spectrom.* **2005,** *16*, 631–646.
19. Patel, T.; Bruce, J.; Merry, A.; Bigge, C.; Wormald, M.; Jaques, A.; Parekh, R. Use of hydrazine to release in intact and unreduced form both N- and O-linked oligosaccharides from glycoproteins. *Biochemistry* **1993,** *32,* 679–693.
20. Wing, D. R.; Field, M. C.; Schmitz, B.; Thor, G.; Dwek, R. A.; Schachner, M. S.; Rademacher, T. W. The use of large-scale hydrazinolysis in the preparation of N-linked oligosaccharide libraries: Application to brain tissue. *Glycoconj. J.* **1992,** *9,* 293–301.
21. de Waard, P.; Koorevaar, A.; Kamerling, J. P.; Vliegenthart, J. F. G. Structure determination by ^{1}H NMR spectroscopy of (sulfated) sialylated *N*-linked carbohydrate chains released from porcine thyroglobulin by peptide-N^4-(*N*-acetyl-β-glucosaminyl)asparagine amidase-F. *J. Biol. Chem.* **1991,** *266,* 4237–4243.
22. Kamerling, J. P.; Rijkse, I.; Maas, A. A. M.; van Kuik, J. A.; Vliegenthart, J. F. G. Sulfated *N*-linked carbohydrate chains in porcine thyroglobulin. *FEBS Letts.* **1988,** *241,* 246–250.
23. Da Silva, M. L. C.; Stubbs, H. J.; Tamura, T.; Rice, K. G. ^{1}H-NMR characterization of a hen ovalbumin tyrosinamide N-linked oligosaccharide library. *Arch. Biochem. Biophys.* **1995,** *318,* 465–475.
24. Harvey, D. J.; Wing, D. R.; Küster, B.; Wilson, I. B. H. Composition of N-linked carbohydrates from ovalbumin and co-purified glycoproteins. *J. Am. Soc. Mass Spectrom.* **2000,** *11,* 564–571.
25. Green, E. D.; Adelt, G.; Baenziger, J. U.; Wilson, S.; van Halbeek, H. The asparagine-linked oligosaccharides on bovine fetuin. Structural analysis of N-glycanase-released oligosaccharides by 500-Megahertz 1H-NMR spectroscopy. *J. Biol. Chem.* **1988,** *263,* 18253–18268.
26. Fournet, B.; Montreuil, J.; Strecker, G.; Dorland, L.; Haverkamp, J.; Vliegenthart, J. F. G.; Binette, J. P.; Schmid, K. Determination of the primary structures of 16 asialo-carbohydrate units derived from human plasma α1-acid glycoprotein by 360 MHz ^{1}H NMR spectroscopy and permethylation analysis. *Biochemistry* **1978,** *17,* 5206–5214.
27. Powell, A. K.; Harvey, D. J. Stabilization of sialic acids in N-linked oligosaccharides and gangliosides for analysis by positive ion matrix-assisted laser desorption-ionization mass spectrometry. *Rapid Commun. Mass Spectrom.* **1996,** *10,* 1027–1032.
28. Domon, B.; Costello, C. E. A systematic nomenclature for carbohydrate fragmentations in FAB-MS/MS spectra of glycoconjugates. *Glycoconj. J.* **1988,** *5,* 397–409.
29. Harvey, D. J.; Martin, R. L.; Jackson, K. A.; Sutton, C. W. Fragmentation of *N*-linked glycans with a MALDI-ion trap time-of-flight mass spectrometer. *Rapid Commun. Mass Spectrom.* **2004,** *18,* 2997–3007.
30. Guile, G. R.; Harvey, D. J.; O'Donnell, N.; Powell, A. K.; Hunter, A. P.; Zamze, S.; Fernandes, D. L.; Dwek, R. A.; Wing, D. R.Identification of highly fucosylated N-linked oligosaccharides from the human parotid gland. *Eur. J. Biochem.* **1998,** *258,* 623–656.
31. Gillece-Castro, B. L.; Prakobphol, A.; Burlingame, A. L.; Leffler, H.; Fisher, S. J. Structure and bacterial receptor activity of a human salivary proline-rich glycoprotein. *J. Biol. Chem.* **1991,** *266,* 17358–17368.
32. Dell, A.; Thomas-Oates, J. E. Fast atom bombardment-mass spectrometry (FAB-MS): Sample preparation and analytical strategies. In *Analysis of Carbohydrates by GLC and MS*; Biermann, C. J.; McGinnis, G. D., Eds.; CRC Press: Boca Raton, 1989; pp 217–235.
33. Garozzo, D.; Impallomeni, G.; Montaudo, G.; Spina, E. Structure of underivatized branched oligosaccharides by negative-ion fast-atom bombardment mass spectrometry. *Rapid Commun. Mass Spectrom.* **1992,** *6,* 550–552.
34. Domon, B.; Müller, D. R.; Richter, W. J. High performance tandem mass spectrometry for sequence, branching and interglycosidic linkage analysis of peracetylated oligosaccharides. *Biomed. Environ. Mass Spectrom.* **1990,** *19,* 390–392.
35. Egge, H.; Peter-Katalinic, J. Fast atom bombardment mass spectrometry for structural elucidation of glycoconjugates. *Mass Spectrom. Rev.* **1987,** *6,* 331–393.
36. Laine, R. A.; Yoon, E.; Mahier, T. J.; Abbas, S.; de Lappe, B.; Jain, R.; Matta, K. Non-reducing terminal linkage position determination in intact and permethylated synthetic oligosaccharides having a penultimate amino sugar: Fast atom bombardment ionization, collision-induced dissociation and tandem mass spectrometry. *Biol. Mass Spectrom.* **1991,** *20,* 505–514.